

Table S1. Animals, Cell Lines, Primers, siRNAs, and Plasmids

Mice			
Description	Strain	Source	
WHAMM ^{HET}	B6N(Cg)- <i>Whamm</i> ^{im1b(KOMP)Wtsi/3J}	The Jackson Laboratory (JR#027472)	
WHAMM ^{WT}	WHAMM ^{WT}	This Study	
WHAMM ^{KO}	WHAMM ^{KO}	This Study	
Cell Lines			
Cell Type	Genotype	Source	
HK-2		ATCC (CRL-2190)	
MEF HET Male	<i>Whamm</i> ^{HET_{XY}}	This Study	
MEF KO Male	<i>Whamm</i> ^{KO_{XY}}	This Study	
Primers			
Description	Species	Sequences	
WHAMM ^{WT}	Mouse	F	GGGCAAGATACAACACTGAA
WHAMM ^{KO}	Mouse	F	CTGGATCCGGAATAACTTCG
WHAMM ^{WT/KO}	Mouse	R	GGCCAGCTTCCTTCTCATAA
SX	Mouse	F	GATGATTTGAGTGAAAATGTGAGGTA
		R	CTTATGTTTATAGGCATGCACCATGTA
GAPDH	Mouse	F	GAGGGCTGCAGTCCGTATTT
		R	CCTCCCCCTATCAGTTCGGA
siRNAs			
Target	Identifier		
Control	Ambion AM4611		
GAPDH	Ambion AM4624		
WHAMM A	Sigma WD07317596		
WHAMM B	Invitrogen HSS151264		
Plasmids			
Description	Vector	Species	Sources
pKC-LAP-C1	N/A	N/A	Campellone <i>et al.</i> , 2008
pKC-LAP-WHAMM	pKC-LAP-C1	Human	Campellone <i>et al.</i> , 2008
pKC-LAP-WHAMM W807A	pKC-LAP-C1	Human	Campellone <i>et al.</i> , 2008

Table S2. Immunofluorescence and Immunoblotting Reagents

Target	Probe	Conc.	Identifier	
Primary Antibodies (Immunofluorescence)				
ACE2	anti-ACE2	Rabbit	1:1,000	Proteintech (21115-I-AP)
Actin	anti- β -Actin	Mouse	1:10,000	Proteintech (66009-I-Ig)
AIF	anti-AIF	Rabbit	1:1,000	Cell Signaling Technology (5318)
GABARAP	anti-GABARAP	Rabbit	1:750	Proteintech (18723-I-AP)
GM130	anti-GM130	Mouse	1:1,000	BD Transduction Laboratories (610822)
LC3	anti-LC3	Rabbit	1:750	Proteintech (14600-I-AP)
LC3B	anti-LC3B	Mouse	1:750	Cell Signaling (83506S)
Megalin	anti-LRP2	Rabbit	1:1,000	Proteintech (19700-I-AP)
Microtubules	anti- β -Tubulin	Mouse	1:1,000	DSHB (E7)
p62	anti-p62	Mouse	1:1,000	BD Transduction Laboratories (610832)
p62	anti-p62/SQSTM1	Rabbit	1:1,000	Proteintech (18420-I-AP)
STX17	anti-Syntaxin 17	Rabbit	1:1,000	Proteintech (17815-I-AP)
Ubiquitin	anti-ubiquitin	Mouse	1:1,000	EDM Millipore (ST1200)
Primary Antibodies (Immunoblotting)				
ACE2	anti-ACE2	Rabbit	1:1,000	Proteintech (21115-I-AP)
Actin	anti-Beta-Actin	Mouse	1:10,000	Proteintech (66009-I-Ig)
GABARAP	anti-GABARAP	Rabbit	1:750	Proteintech (18723-I-AP)
GAPDH	anti-GAPDH	Mouse	1:10,000	Proteintech (60004-I-Ig)
LC3	anti-LC3	Rabbit	1:750	Proteintech (14600-I-AP)
Megalin	anti-LRP2	Rabbit	1:1,000	Proteintech (19700-I-AP)
SGLT2	anti-SGTL2	Rabbit	1:1,000	Proteintech (24654-I-AP)
SLC20A1	anti-SLC20A1	Rabbit	1:1,000	Proteintech (12423-I-AP)
Tubulin	anti- β -Tubulin	Mouse	1:10,000	DSHB (E7)
WHAMM	anti-WHAMM	Rabbit	1:1,000	Shen <i>et al.</i> , 2012
Secondary Antibodies (Immunofluorescence)				
Mouse IgG	Alexa 488, 555 anti-mouse	Goat	4 μ g/mL	Life Technologies (A11029; A21424)
Rabbit IgG	Alexa 488 anti-rabbit	Goat	4 μ g/mL	Life Technologies (A11034)
Secondary Antibodies (Immunoblotting)				
Mouse IgG	IRDye 680 anti-Mouse	Donkey	0.5 μ g/mL	LI-COR (926-68022)
Rabbit IgG	IRDye 800 anti-Rabbit	Donkey	0.5 μ g/mL	LI-COR (926-32213)
Rabbit IgG	HRP anti-Rabbit	Donkey	1:10,000	GE Healthcare (NA934V)
Molecular Probes (Fluorescence)				
DNA	4',6-diamidino-2-phenylindole (DAPI)		1 μ g/mL	Invitrogen (D1306)
F-actin	AlexaFluor 647-Phalloidin		0.4 U/mL	Invitrogen (A22287)

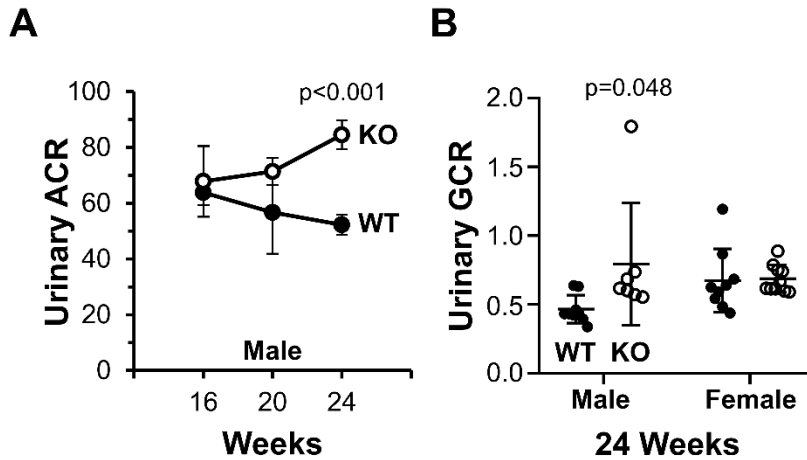


Figure S1. Male WHAMM^{KO} mice excrete elevated levels of urinary albumin and glucose. (A) Urine samples were collected from male wild type (WT; filled circles) or WHAMM knockout (KO; open circles) mice. Urinary albumin-to-creatinine ratios (ACR) for males from 16 to 24 weeks-of-age were plotted. Each circle represents the mean \pm SE from n=6-7 mice per genotype for each timepoint. (B) Urinary glucose-to-creatinine ratios (GCR) from male and female mice were plotted. Each circle represents one mouse. Statistical bars display the mean \pm SD from n=7-9 mice. Significant p-values are noted (unpaired t-tests).

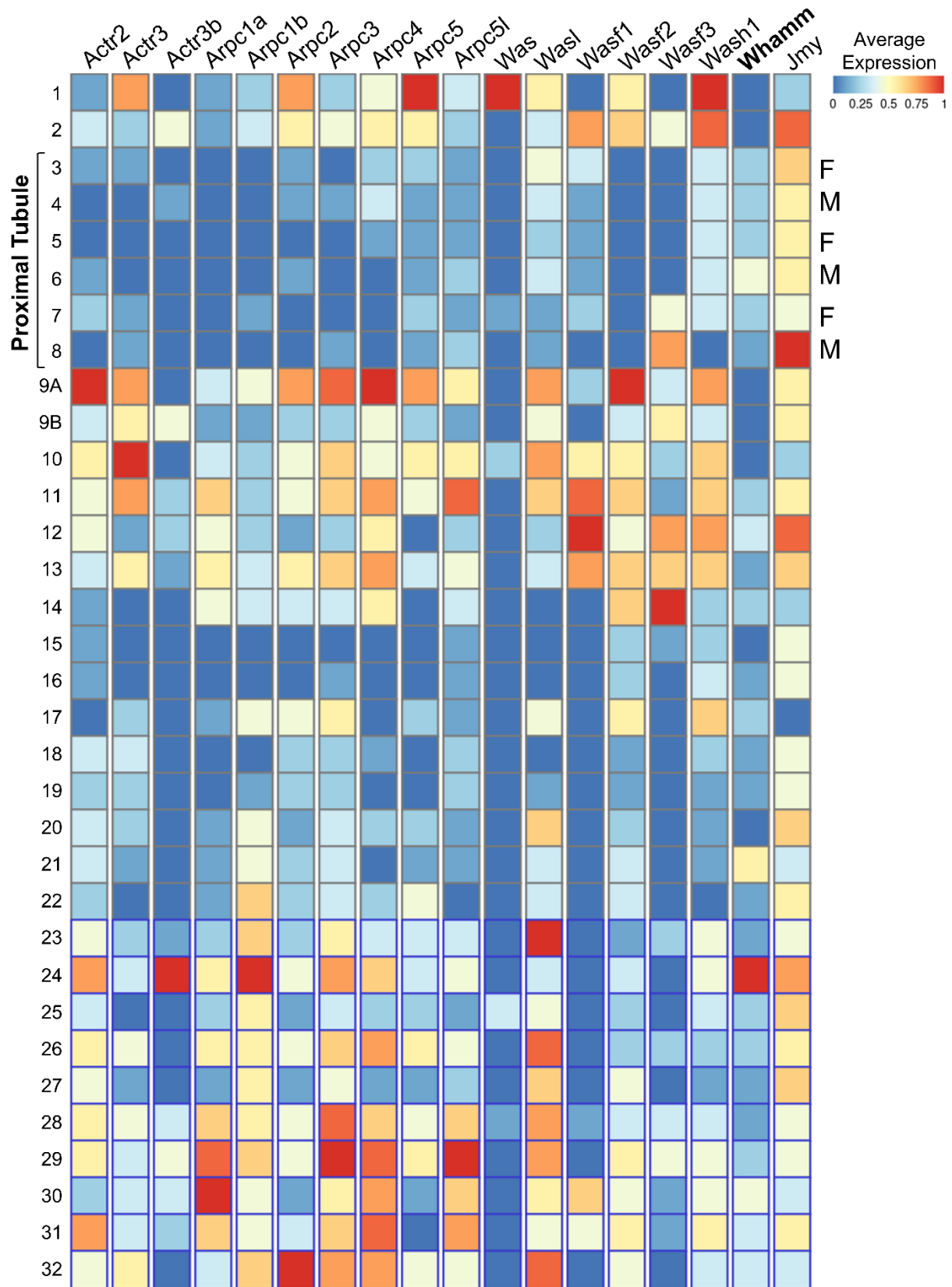


Figure S2. Average relative expression of Arp2/3 complex subunits and WASP-family genes in the nephron. Data from KidneyCellExplorer (cello.shinyapps.io/kidneycellexplorer; (Ransick *et al.*, 2019)) is based on single-cell RNA sequencing analyses and grouping into “metacell” clusters for mouse nephron regions 1-32. Average expression is plotted on a 0-1 scale and displayed in a heat map, wherein 0 represents no expression for a particular gene and 1 is assigned to the region of the nephron in which that gene’s expression is highest. Abbreviations: 1 – Podocytes; 2 – Parietal epithelium; 3 – Segment 1 Proximal Tubule (Female); 4 – Segment 1 Proximal Tubule (Male); 5 – Segment 2 Proximal Tubule (Female); 6 – Segment 2 Proximal Tubule (Male); 7 – Segment 3 Proximal Tubule (Female); 8 – Segment 3 Proximal Tubule (Male); 9A – LOH thin descending limb of inner stripe of outer medulla of cortical nephron; 9B – LOH thin descending limb of inner stripe of outer medulla of juxtamedullary nephron; 10 – Upper LOH thin descending limb of inner medulla of juxtamedullary nephron; 11 – Lower LOH thin descending limb of inner medulla of juxtamedullary nephron; 12 – Lower LOH thin limb of inner medulla of juxtamedullary nephron; 13 – Lower LOH thin limb of inner medulla of juxtamedullary nephron; 14 – Upper LOH thin ascending limb of inner medulla of juxtamedullary nephron; 15 – Distal straight tubule of inner stripe of outer medulla; 16 – Distal straight tubule of outer stripe of outer medulla and cortex; 17 – Macula densa; 18 – Distal convoluted tubule; 19 – Nephron connecting tubule; 20 – Principal-like cell of nephron connecting tubule; 21 – Intercalated type non-A non-B cell of nephron connecting tubule; 22 – Intercalated type A cell of nephron connecting tubule and cortical collecting duct; 23 – Principal-like cell of cortical collecting duct; 24 – Intercalated type B cell of cortical collecting duct; 25 – Intercalated type A cell of outer medullary collecting duct; 26 – Principal cell of outer medullary collecting duct; 27 – Intercalated type A cell of inner medullary collecting duct; 28 – Principal cell of inner medullary collecting duct type 1; 29 – Principal cell of inner medullary collecting duct type 2; 30 – Principal-like cell of deep inner medullary collecting duct type 1; 31 – Cell of deep inner medullary collecting duct type 2; 32 – Deep medullary epithelium of pelvis.

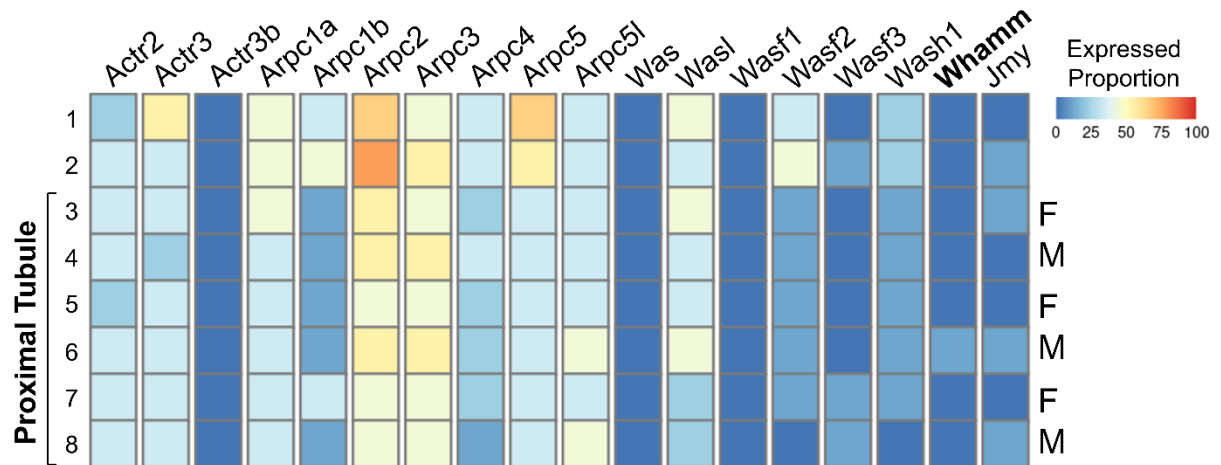


Figure S3. Proportion of cells expressing Arp2/3 complex subunits and WASP-family genes in the nephron. Data from KidneyCellExplorer (cello.shinyapps.io/kidneycellexplorer; (Ransick *et al.*, 2019)) is based on single-cell RNA sequencing analyses and grouping into “metacell” clusters for mouse nephron regions 1-32 as in Figure S2. The proportion of cells expressing a gene of interest in each metacell is plotted on a 0-100 scale and displayed according to the heat map.

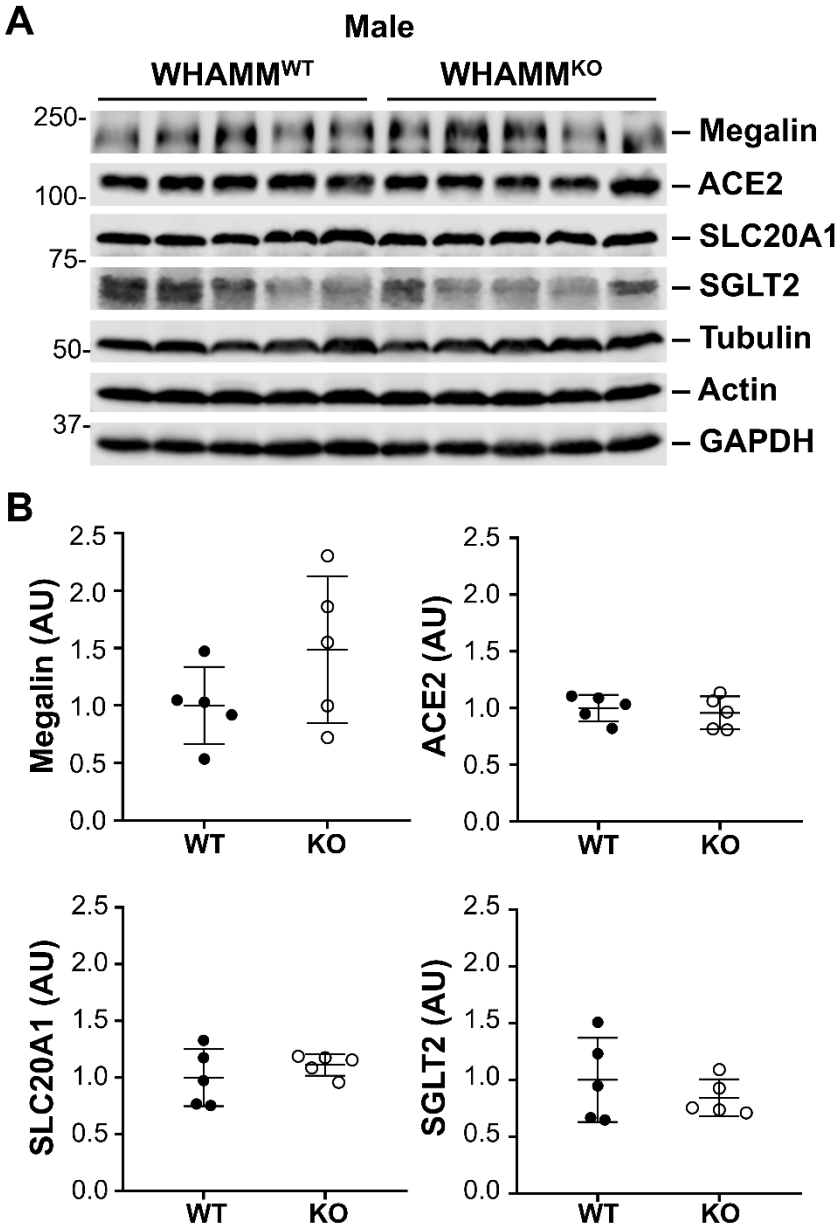


Figure S4. Expression of several plasma membrane receptors is similar in male WHAMM^{WT} and WHAMM^{KO} kidneys. (A) Kidney extracts from 5 male wild type (WHAMM^{WT}) and 5 WHAMM knockout (WHAMM^{KO}) mice were processed, and 50 μ g samples were subjected to SDS-PAGE and immunoblotted with antibodies to Megalin, ACE2, SLC20A1, SGLT2, tubulin, actin, and GAPDH. (B) Band intensities for the receptors in (A) were quantified relative to tubulin, actin, and GAPDH, and the normalized values were plotted. Each circle represents one mouse. Statistical bars represent the mean \pm SD from n=5 mice.

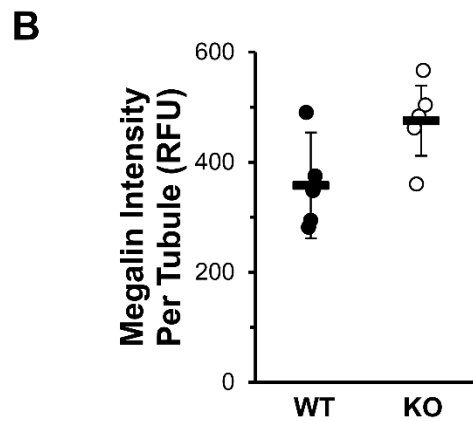
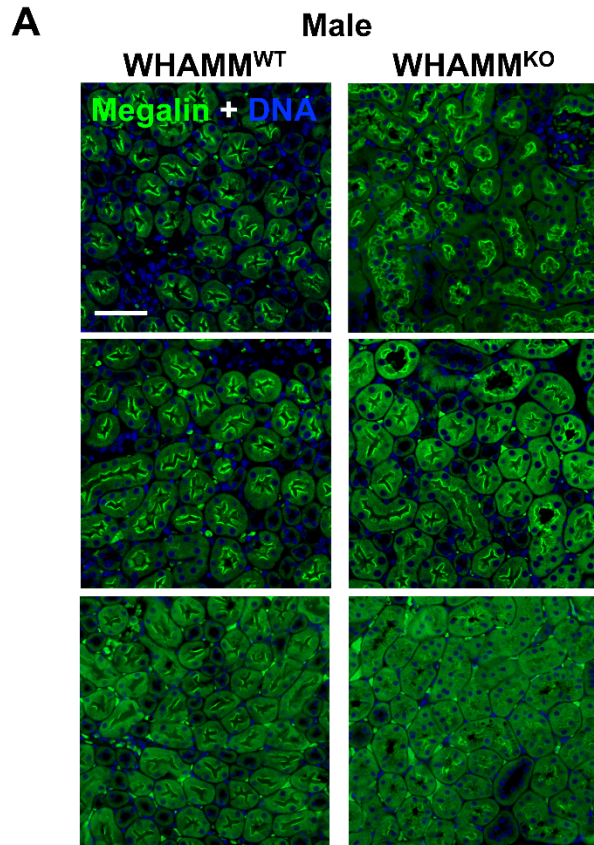


Figure S5. Megalin localization and expression in kidneys from WHAMM^{WT} and WHAMM^{KO} mice. (A) Kidney tissue sections from WHAMM^{WT} or WHAMM^{KO} male mice were stained with Megalin antibodies (green) and DAPI (DNA; blue). Scale bar, 50 μ m. **(B)** The Megalin fluorescence intensity per tubule was calculated in ImageJ. Each circle represents Megalin kidney staining from an individual mouse in which approximately 60 tubules were examined. Statistical bars represent the mean \pm SD from n=5 kidneys.

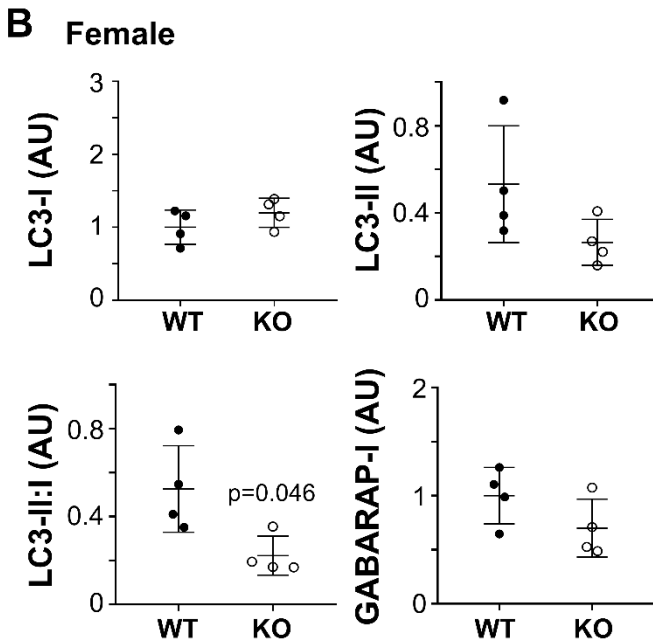
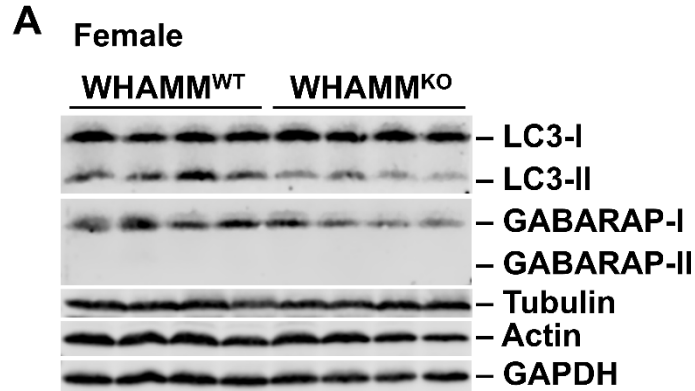


Figure S6. The LC3 II:I ratio is slightly decreased in female WHAMM^{KO} kidneys. (A) Kidney extracts from 4 female WHAMM^{WT} and 4 female WHAMM^{KO} mice were processed, and 50 μ g samples were subjected to SDS-PAGE and immunoblotted with antibodies to LC3, GABARAP, tubulin, actin, and GAPDH. **(B)** LC3 and GABARAP band intensities were quantified relative to tubulin, actin, and GAPDH, and the mean normalized values were plotted. The LC3-II:I ratio was calculated by dividing the LC3-II band intensity by the LC3-I band intensity within each non-normalized sample. Each circle represents one mouse. Statistical bars represent the mean \pm SD from n=5 mice. A significant p-value is noted (unpaired t-test).

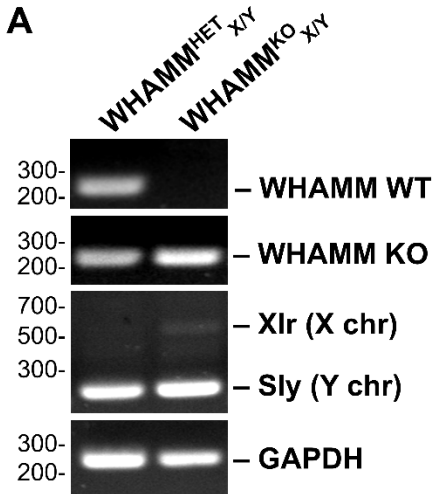
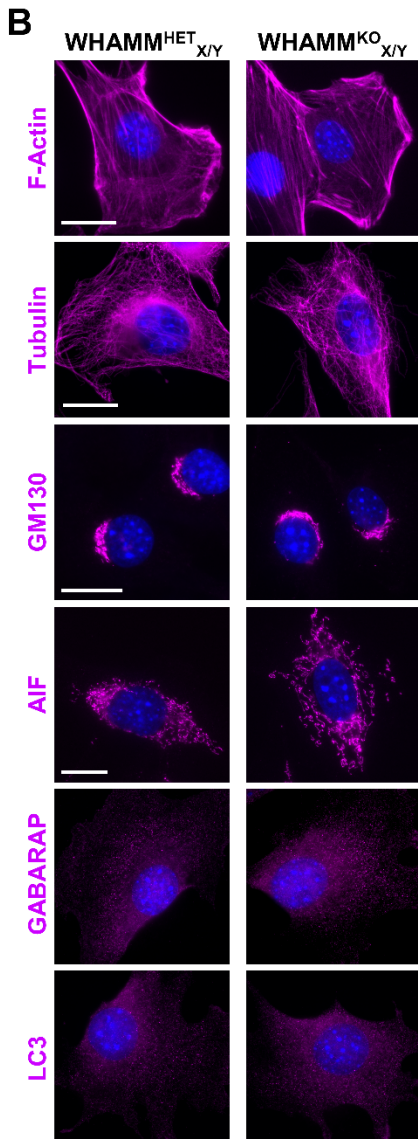


Figure S7. Genotyping and microscopic analyses of mouse embryonic fibroblasts. (A) Genomic DNA was isolated from mouse embryonic fibroblasts (MEFs) and subjected to PCR with primers to wild type *Whamm* (WHAMM WT), mutant *Whamm* (WHAMM KO), *Sly* (Y chromosome)/*Xlr* (X chromosome), and *Gapdh*, and visualized following agarose gel electrophoresis. (B) Male heterozygous (WHAMM^{HET}_{X/Y}) and male knockout (WHAMM^{KO}_{X/Y}) MEFs were fixed and stained with phalloidin to visualize F-actin or with antibodies to visualize microtubules (Tubulin), the *cis*-Golgi (GM130), mitochondria (AIF), or autophagosomes (LC3, GABARAP) each shown in magenta. DAPI-stained nuclei are shown in blue. Scale bar, 20 μ m. Despite multiple attempts, we were unable to isolate male wild type MEFs.



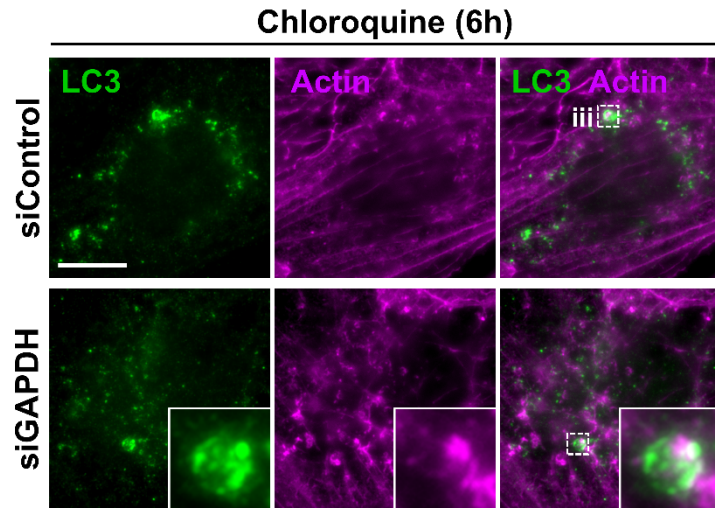


Figure S8. Actin localizes to autophagosomes in proximal tubule cells. HK-2 cells were treated with Control or GAPDH siRNAs and exposed to media containing chloroquine before being fixed and stained with antibodies to LC3 (green) and actin (magenta). Scale bar, 10 μ m. The magnification of (iii) is shown in Figure 3C.

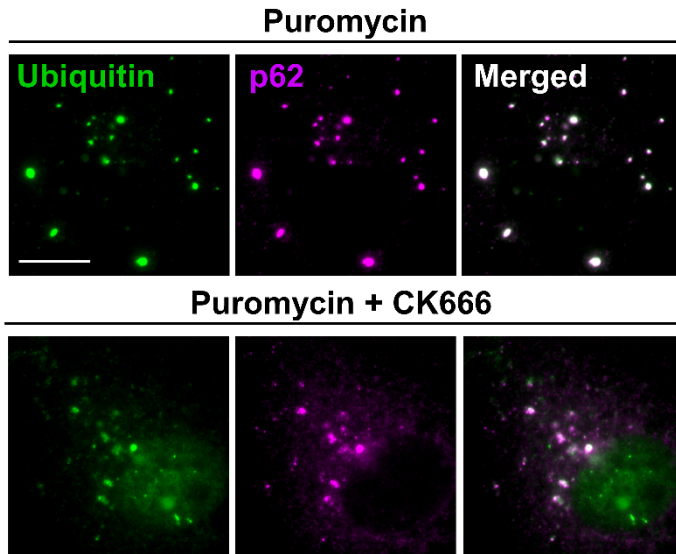


Figure S9. Arp2/3 complex inhibition does not prevent the recruitment of p62 to ubiquitinated protein aggregates following proteotoxic stress. HK-2 cells were treated with puromycin or puromycin plus CK666 for 2h before being fixed and stained with antibodies to ubiquitin (green) and p62 (magenta). Scale bar, 10 μ m. Exposure to puromycin increased the formation of bright, ubiquitin and p62-stained foci. Cells co-treated with puromycin and CK666 also harbored diffuse cytoplasmic ubiquitin and p62 staining, consistent with previous findings that the Arp2/3 complex is important for the formation of p62 bodies (Feng *et al.*, 2022). While the Arp2/3 complex may affect the coalescence of ubiquitin- and p62-bound cargo, it is not required for the recruitment of p62 to ubiquitinated material.